Identification of Dynamic Mass Spring Parameters for Deformable Body Simulation

B. A. Lloyd and S. Kirac and G. Székely and M. Harders

Computer Vision Laboratory, ETH Zürich, Switzerland

Abstract

Mass spring systems (MSS) are frequently used to simulate deformable objects because of their conceptual simplicity and computational speed. Unfortunately, the model parameters (spring coefficients, masses) are not related to material constitutive laws in an obvious way. In our earlier work we proposed a method, which can be used to relate the parameters of the MSS to constitutive models, often used in continuum mechanics. In this report we have used this strategy to develop new formulae for the dynamic MSS parameters, i.e. the masses and the damping coefficients. This is the first report which identifies the damper coefficients analytically. In this work we restrict our attention to triangular meshes. Experimental evidence is given in support of our results.

1. Introduction

Mass spring systems (MSS) [TPBF87] are frequently used to simulate deformable objects because of their conceptual simplicity and computational speed. Typical example applications are cloth animation and simulation of facial expressions [BW98, KHS01]. Unfortunately, the model parameters (spring coefficients, masses) are not related to elastic material constitutive laws in an obvious way. In our recent article we proposed a method, which relates the parameters of the MSS to constitutive models, often used in continuum mechanics [LSH07]. Most measured material properties are documented in terms of the parameters found in these constitutive laws. Our approach allows this existing knowledge to be applied in mass spring simulations. The derivation of stiffness coefficients for several 2D and 3D mesh topologies was shown and validated. In the current work we have applied the same approach to determine the masses and damping constants of a Kelvin-Voigt type damped mass spring model, taking an isotropic linear elastic material with first order Rayleigh damping as a reference [LG95]. The strategy we follow is to compare the force balance equation of the MSS with the equivalent equation obtained with a finite element method. A coefficient comparison then results in formulae for the MSS parameters.

Our previous paper was motivated by and extended the work of Van Gelder [Gel98]. These approaches were, however, limited to the static case and provided estimates for the spring stiffness coefficients. There have been few reports describing how the dynamic parameters should be estimated/chosen. We are aware of only one paper by Paloc et al. [PBKD02], where an estimate of the magnitude of the spring damping coefficient, depending on the damping ratio, is provided. Some further work has also been performed on iteratively setting node masses based on Voronoi diagrams [DKT95] and parameter identification for dynamic simulation [JGL97]. For a more detailed overview of the literature, we refer the reader to [LSH07].

2. Methods

2.1. Finite Element Equations

In the FEM the continuous model is discretized by dividing the object into small interconnected regions, called finite elements. The constitutive laws are approximated by interpolation functions associated with each element. A commonly used 2D element is the constant strain triangle, also called 3-node triangle with linear displacement interpolation functions. The dynamic equations of motion are

$$M_{FEM}\,\ddot{\mathbf{d}} + D_{FEM}\,\dot{\mathbf{d}} + K_{FEM}\,\mathbf{d} = \mathbf{f}, \qquad (1)$$

where $\mathbf{f}$ is a vector containing the forces at the three nodes, $\mathbf{d}$ are the node displacements due to the forces $\mathbf{f}$, K_{FEM} is the stiffness, M_{FEM} the mass and D_{FEM} the damping matrix. Throughout this paper we follow the convention that force and displacement vectors are ordered by node. The 6×6

symmetric element stiffness matrix can be computed analytically. An expression for the plane stress stiffness matrix in terms of the node coordinates and material parameters can be found in [LSH07] and will not be repeated here. A FEM derivation of the mass matrix results in a non-diagonal structure. However, very often a diagonal approximation, called a lumped mass matrix, is chosen [ZT00] : $M_{FEM} = \left(\frac{Ah}{3}\right) \rho I_6$, where I_6 is a 6×6 identity matrix, A is the area of the triangle, h is its thickness and ρ is the mass density. Basically, the mass of the element is equally distributed to each node. This form has major computational advantages, without introducing severe errors. Since damping is only partly understood, there are only few models based on first principles. A commonly chosen damping matrix relies on the generalized Rayleigh model

$$D_{FEM} = M_{FEM} \sum_{i=0}^{N} \alpha_i (M_{FEM}^{-1} K_{FEM})^i, \tag{2}$$

where α_i are the model parameters [LG95]. We use the first order form $D_{FEM} = \alpha_0 M_{FEM} + \alpha_1 K_{FEM}$.

2.2. Linearized Mass Spring Model Equations

We choose a triangle MSS consisting of the nodes $\mathbf{p}_i$, $\mathbf{p}_j$ and $\mathbf{p}_k$ connected by three springs as the corresponding model. The edges of the triangle are assumed to correspond to springs. The mass is distributed at the nodes. In this section we linearize the model and derive its stiffness, damping and mass matrices. The dynamic equation of motion for a connected mass spring system at a node i is

$$m_i \ddot{\mathbf{d}}_i + \mathbf{f}_i^{int}(\mathbf{d}_i, \dot{\mathbf{d}}_i) = \mathbf{f}_i^{ext}, \tag{3}$$

where m_i is the mass at node i and $\mathbf{f}_i^{int}$ are the internal forces. In order to compare the MSS with the linear visco-elastic material model, we re-write the force equation in matrix notation. For an assembly of springs, it can easily be seen that the mass matrix is diagonal, i.e. in the case of a triangle MSS

$$M_{MSS} = \begin{bmatrix} m_i I_2 & 0 & 0 \\ 0 & m_j I_2 & 0 \\ 0 & 0 & m_k I_2 \end{bmatrix}. \tag{4}$$

The internal force at node i is the sum of an elastic force $\mathbf{f}^s$ and a viscous force $\mathbf{f}^d$

$$\mathbf{f}_i^s = \sum k_{ij} \left[(\mathbf{p}_i - \mathbf{p}_j) \left(1 - \frac{l_{ij}^0}{\|\mathbf{p}_i - \mathbf{p}_j\|} \right) \right]$$

$$\mathbf{f}_i^d = \gamma_i^d \dot{\mathbf{p}}_i + \sum \gamma_{ij} \left\langle (\dot{\mathbf{p}}_i - \dot{\mathbf{p}}_j), \frac{(\mathbf{p}_i - \mathbf{p}_j)}{\|\mathbf{p}_i - \mathbf{p}_j\|} \right\rangle \frac{(\mathbf{p}_i - \mathbf{p}_j)}{\|\mathbf{p}_i - \mathbf{p}_j\|}$$

where $N(i)$ is the set of springs connected to node i and $\mathbf{p}_i = (x_i, y_i)^T$ is the position of node i. The variables k_{ij} and l_{ij}^0 correspond to the spring coefficient and rest-length respectively. The parameters γ_i^d and γ_{ij} are point and spring damping coefficients respectively. In [LSH07] the linearization of the undamped spring force (elastic part) was shown to be

$$\begin{pmatrix} \mathbf{f}_i^s \\ \mathbf{f}_j^s \end{pmatrix} \cong K_{S_{i,j}} \begin{pmatrix} \mathbf{d}_i \\ \mathbf{d}_j \end{pmatrix} \tag{5}$$

$$K_{S_{i,j}} = k_{ij} \begin{bmatrix} A_{ij} & -A_{ij} \\ -A_{ij} & A_{ij} \end{bmatrix} \tag{6}$$

where

$$A_{ij} = \frac{1}{l_{ij}^{0\,2}} (\mathbf{p}_i - \mathbf{p}_j)(\mathbf{p}_i - \mathbf{p}_j)^T. \tag{7}$$

The damping force term (viscous part) is linear in the node velocities and, therefore, can easily be re-written in matrix form.

$$\begin{pmatrix} \mathbf{f}_i^d \\ \mathbf{f}_j^d \end{pmatrix} = (D^p + D^s) \begin{pmatrix} \dot{\mathbf{p}}_i \\ \dot{\mathbf{p}}_j \end{pmatrix} = \left(\begin{bmatrix} \gamma_i^d I_2 & 0 \\ 0 & \gamma_j^d I_2 \end{bmatrix} + \gamma_{ij} \begin{bmatrix} A_{ij} & -A_{ij} \\ -A_{ij} & A_{ij} \end{bmatrix} \right) \begin{pmatrix} \dot{\mathbf{p}}_i \\ \dot{\mathbf{p}}_j \end{pmatrix}. \tag{8}$$

Note that the matrix in the first term (point damping) is diagonal, while the matrix in the second term (spring damping) turns out to be proportional to the spring stiffness matrix $K_{S_{i,j}}$ (Equation 6). We obtain the stiffness matrix of a triangle MSS by summing the stiffness matrices of each spring (since forces add). Introducing the variable $\hat{A}_{ij} = k_{ij} A_{ij}$ for notational simplicity, the stiffness matrix is

$$K_{MSS} = \sum_{l,m} K_{S_{l,m}} = \begin{bmatrix} \hat{A}_{ij} + \hat{A}_{ik} & -\hat{A}_{ij} & -\hat{A}_{ik} \\ -\hat{A}_{ij} & \hat{A}_{ij} + \hat{A}_{jk} & -\hat{A}_{jk} \\ -\hat{A}_{ik} & -\hat{A}_{jk} & \hat{A}_{ik} + \hat{A}_{jk} \end{bmatrix}. \tag{9}$$

where the summation is done in global coordinates. Since each sub-matrix A_{ij} is symmetric, the stiffness matrix of the triangle model is also symmetric. The assembly of the damping matrix is analogous and will be skipped. Finally, using the derived terms, we can write (the linearized) equations of motion in matrix notation

$$M_{MSS} \ddot{\mathbf{d}} + D_{MSS} \dot{\mathbf{d}} + K_{MSS} \mathbf{d} = \mathbf{f}. \tag{10}$$

2.3. Coefficient Comparison

The dynamic equations of motion derived using a FEM and the linearized MSS contain the same variables, i.e. the node displacements, velocities and accelerations. The same dynamical behavior for FEM and MSS simulations should result, if the coefficients are equal in both equations. In addition to equating the stiffness matrices as in [LSH07], we now also compare the mass and the damping matrices. It is already known that the stiffness matrices are equal under certain conditions. From this relation it was derived that the spring stiffness coefficient is

$$k_{ij} = \sum_e E h \frac{\sqrt{3}}{4}. \tag{11}$$

Comparison of the mass matrices gives us the mass parameter for the MSS

$$m_i = \sum_e \frac{A_e h}{3} \rho, \tag{12}$$

where the sum is taken over the adjacent triangles, h is the thickness of the thin layer and ρ is the mass density. Finally, the comparison between the Rayleigh damping matrix used in the FEM and the MSS damping matrix obtained from point damping combined with spring damping results in following damping coefficients

$$\gamma_i^d = \alpha_0 \sum_e \frac{A_e h}{3} \rho \quad \gamma_{ij} = \alpha_1 \sum_e E h \frac{\sqrt{3}}{4}. \tag{13}$$

3. Results

In order to verify the theoretical results we have used the formulae to simulate several deformation examples, for different damping coefficients. The time integration for the MSS was performed with a Verlet scheme [THMG04]. The computed deformations were compared to a FEM simulation performed with a commercial solver. First a mesh was constructed using only equilateral triangles, since the spring stiffness coefficient presented in [LSH07] is derived under this assumption. Then, however, we also simulated deformations using non-equilateral triangles, in order to test if the results are valid in a more general sense. The test cases simulate the deformation of a rectangular membrane, which at time zero suddenly is exposed to a body force. The object is attached at the bottom ($y = 0$) and if not specified differently the body force is directed in negative y-direction.

Only a small mass damping was chosen for the first experiment (just large enough to assure stability). Within the simulated time, the amplitude does not decay noticeably. The comparative results are shown in Figure 1. Although

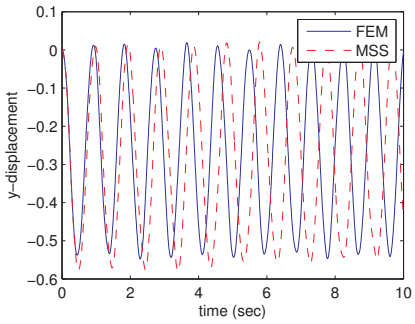

Figure 1: *Object oscillating after applying a body force in negative y-direction, causing a compression of up to* 15%.

the amplitudes of the MSS and the FEM are approximately equal over time, there is a noticeable phase shift between the two models. The relative difference between the oscillatory periods T_{MSS} and T_{FEM} is approximately 5% for this example ($T_{MSS} \simeq 1.055\, T_{FEM}$). The reason for this is mentioned in [LSH07]. The MSS has a non-linear stiffness curve - it is softer under directed compression, and stiffer when stretched. A softer material will oscillate at a smaller frequency f, since $f \propto \sqrt{\frac{E}{\rho}}$. Therefore, we can expect the period of the MSS to be smaller than the FE model, when elongated. This is indeed the case as shown in Figure 2 a)($T_{MSS} \simeq 0.975\, T_{FEM}$). The frequency shift is due to the

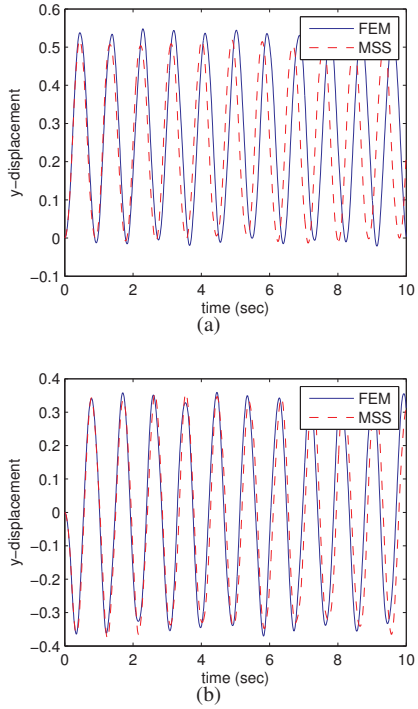

Figure 2: *Object oscillating after applying a body force in positive y-direction, effectively stretching the object up to* 15%.

fact the mean deformation is not in the position, where the operating point linearization was done (i.e. in the rest position). We have verified this in Figure 2 b) by applying a force for only a short period of time (pulse), such that the mean deformation in the subsequent oscillation is close to zero. As a next step, the influence of damping on the results have been investigated. In Figure 3 we simulated the effect of mass damping ($\alpha_0 = 1.0$, $\alpha_1 = 0$). Note how the amplitude decays at the same rate in both the MSS and the finite element simulation. For the experiment shown in Figure 4 spring damping was applied using $\alpha_1 = 0.01$ and $\alpha_0 = 0$. The decay of the amplitude was again very similar in both the MSS and the finite element simulation. Finally, the quality of the approximation has also been tested on models consisting of non-equilateral triangles, i.e. meshed with an arbitrary meshing tool. The results of the simulations with either point damping or spring damping are shown in Figures 5 a)

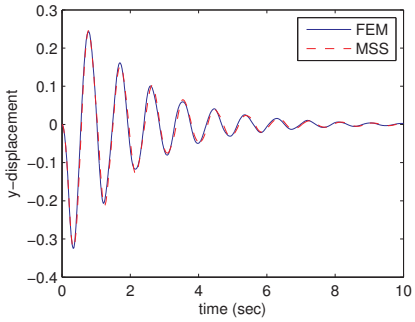

Figure 3: *A force is applied in negative y-direction for* 0.2*sec. Mass damping is tested using the parameters* $\alpha_0 = 1.0$ *and* $\alpha_1 = 0$.

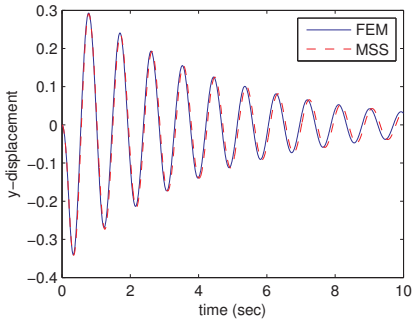

Figure 4: *A force is applied in negative y-direction for* 0.2*sec. Structural (spring) damping is tested using the parameters* $\alpha_0 = 0$ *and* $\alpha_1 = 0.01$.

and b) respectively. Again a force impulse was applied for a

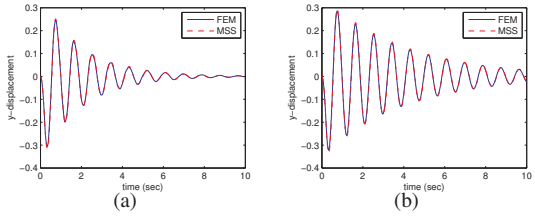

Figure 5: *In Figure a) point damping (*$\alpha_0 = 1.0$*) was tested. In b) spring damping is shown for* $\alpha_1 = 0.01$.

short time, in order to generate an oscillation. Equally convincing results were obtained for different mesh resolutions.

4. Conclusions and Future Work

We have presented formulae for the dynamic parameters of a MSS, which relate to the physical constitutive laws from continuum mechanics. This is the first report which identifies the damper coefficients analytically. Experimental evidence is given in support of our results. One finding in the experiments is that the non-linearity of the MSS causes a oscillation frequency shift, which depends on the kind of deformation (stretch, compression). In this sense the derived formulae provide a best mean estimate. In the near future we would like to use this or a similar strategy to create nonlinear mass spring systems, which are related to known hyperelastic material constitutive laws.

Acknowledgment: This work has been performed within the frame of the Swiss National Center of Competence in Research on Computer Aided and Image Guided Medical Interventions (NCCR Co-Me) supported by the Swiss National Science Foundation. We would like to thank Andreas Griesser for his help with the movie.

References

[BW98] BARAFF D., WITKIN A.: Large steps in cloth simulation. In *SIGGRAPH '98: Proceedings of the 25th annual conference on Computer graphics and interactive techniques* (New York, NY, USA, 1998), ACM Press, pp. 43–54.

[DKT95] DEUSSEN O., KOBBELT L., TUCKE P.: Using simulated annealing to obtain good nodal approximations of deformable objects. In *Computer Animation and Simulation* (1995), pp. 30–43.

[Gel98] GELDER A. V.: Approximate simulation of elastic membranes by triangulated spring meshes. *J. Graph. Tools 3*, 2 (1998), 21–42.

[JGL97] JOUKHADAR A., GARAT F., LAUGIER C.: Parameter identification for dynamic simulation. In *Robotics and Automation, IEEE International Conference on* (1997), pp. 1928–1933.

[KHS01] KÄHLER K., HABER J., SEIDEL H.-P.: Geometry-based muscle modeling for facial animation. In *Proceedings of Graphics Interface* (2001), Canadian Information Processing Society, pp. 37–46.

[LG95] LIU M., GORMAN D. G.: Formulation of rayleigh damping and its extensions. *Computers & Structures 57*, 2 (Oct. 1995), 277–285.

[LSH07] LLOYD B. A., SZÉKELY G., HARDERS M.: Identification of spring parameters for deformable object simulation. *Visualization and Computer Graphics, IEEE Transactions on 13* (2007), 1081–1094.

[PBKD02] PALOC C., BELLO F., KITNEY R. I., DARZI A.: Online multiresolution volumetric mass spring model for real time soft tissue deformation. In *MICCAI* (2002), Springer-Verlag, pp. 219–226.

[THMG04] TESCHNER M., HEIDELBERGER B., MÜLLER M., GROSS M.: A versatile and robust model for geometrically complex deformable solids. In *Proc. of the Computer Graphics International* (2004), pp. 312–319.

[TPBF87] TERZOPOULOS D., PLATT J., BARR A., FLEISCHER K.: Elastically deformable models. *SIGGRAPH Comput. Graph. 21*, 4 (1987), 205–214.

[ZT00] ZIENKIEWICZ O., TAYLOR R.: *The Finite Element Method, Volume 1 - The Basics*. Elsevier, 2000.